



Research article

Rapid measurement of bacterial contamination in water: A catalase responsive-electrochemical sensor

Arti Sharma¹, Akanksha Mishra¹, Meenu Chhabra^{*}*Environmental Biotechnology Laboratory, Department of Bioscience and Bioengineering, Indian Institute of Technology Jodhpur (IITJ), Jodhpur, 342030, Rajasthan, India*

ARTICLE INFO

Keywords:

Bacterial sensor
Potentiometric response
Coliforms
Hydrogen peroxide
Electrochemical reactions
Catalase reaction

ABSTRACT

The present study describes the development of a potentiometric sensor for microbial monitoring in water based on catalase activity. The sensor comprises a MnO₂-modified electrode that responds linearly to hydrogen peroxide (H₂O₂) from 0.16 M to 3.26 M. The electrode potential drops when the H₂O₂ solution is spiked with catalase or catalase-producing microorganisms that decompose H₂O₂. The sensor is responsive to different bacteria and their catalase activities. The electrochemical sensor exhibits a lower limit of detection (LOD) for *Escherichia coli* at 11 CFU/ml, *Citrobacter youngae* at 12 CFU/ml, and *Pseudomonas aeruginosa* at 23 CFU/ml. The sensor shows high sensitivity at 3.49, 3.02, and 4.24 mV/cm²dec for *E. coli*, *C. youngae*, and *P. aeruginosa*, respectively. The abiotic sensing electrode can be used multiple times without changing the response potential (up to 100 readings) with a shelf-life of over six months. The response time is a few seconds, with a total test time of 5 min. Additionally, the sensor effectively tested actual samples (drinking and grey water), which makes it a quick and reliable sensing tool. Therefore, the study offers a promising water monitoring tool with high sensitivity, stability, good detection limit, and minimum interference from other water contaminants.

1. Introduction

Since the majority of water-borne illnesses are caused by pathogenic bacteria present in contaminated water, appropriate disinfection should be performed before its consumption. Even at very low levels, bacterial contamination is harmful. The American Public Health Association (APHA) has described the limit of coliforms in drinking water as zero CFU/100 ml [1]. Coliforms are considered as water quality indicators which includes *Escherichia coli*, *Citrobacter youngae*, etc. *Pseudomonas* is another catalase-positive bacterial group present in contaminated water. *E. coli* contamination in water represents fecal contamination, while *Pseudomonas* primarily enters into water through hospital wastes [2–4]. The direct detection of bacteria usually takes several hours, but assays based on bacterial enzymes are quick and accurate. Catalase is one such enzyme that serves as a useful water quality indicator. Microbial activity and biochemical oxygen demand (BOD) are highly associated with catalase activity in water [5,6]. Catalase decomposes hydrogen peroxide (H₂O₂) into H₂O and O₂. Conventionally, the catalase test involves adding a drop of bacterial culture to an H₂O₂ (0.98 M) solution, and observing the formation of O₂ bubbles [7]. However, it provides qualitative results only, and specific laboratory assays are required to measure catalase concentrations accurately [8].

^{*} Corresponding author. IIT Jodhpur, Rajasthan, 342030, India.

E-mail address: meenuchhabra@iitj.ac.in (M. Chhabra).

¹ Both authors AS and AM contributed equally to this work.

<https://doi.org/10.1016/j.heliyon.2024.e26724>

Received 13 February 2024; Received in revised form 19 February 2024; Accepted 19 February 2024

Available online 21 February 2024

2405-8440/Â© 2024 Published by Elsevier Ltd. This is an open access article under the CC BY-NC-ND license (<http://creativecommons.org/licenses/by-nc-nd/4.0/>).

The H_2O_2 concentration can be measured electrochemically using suitable electrode preparations. In certain cases, biosensors make use of immobilized catalase enzymes to sensitively measure H_2O_2 [9–11]. In all these studies, catalase aids in H_2O_2 sensing, but the reverse has not been tested. In many studies, nanomaterial-based sensors are developed for sensitive determination of H_2O_2 , which involves the use of Fe@G-MWCNT, birnessite manganese oxide (MnO_2) decorated MWCNT, $\text{MnO}_2/\text{VACNTs}$, or ultra-thin/nano MnO_2 sheets [12–15]. Graphite felt is commonly used in bio-electrochemical cells for its high surface area, high conductivity, biocompatibility, and relatively lower price [16]. Previous studies have used electrode modification with MnO_2 for enhanced electrode reactivity [17–20]. Treatment with MnO_2 increases the electrode surface area and redox reactions with test compounds. The later allows the detection of test compounds [21]. MnO_2 has the highest catalytic activity for the degradation of H_2O_2 among other transition metal oxides [22,23]. It also regenerates its original oxidation state by interacting with carbon electrodes [24]. This cyclic response enables repeated electrode use with reproducible results [25].

Nevertheless, the studies have demonstrated the H_2O_2 sensing with biotic or abiotic electrodes. However, none of the investigations make an association between H_2O_2 sensing and bacterial monitoring in water. Studies that describe the bacterial detection in water by electrochemical means generally use complicated electrode configurations and measurements that usually depend on amperometry, conductometry, or impedance. For the signal acquisition in these tests, additional electrochemical components are needed, which increases response time and lowers LOD. For example, platinum wire electrodes modified with organic/inorganic-hybrid sol-gel films were used to electrochemically monitor *E. coli*. The sol-gel film was composed of organosilanes, chitosan, and bovine serum albumin. The sensor took a minimum 60 min to respond [26]. Additionally, Serra et al. have demonstrated bacterial monitoring using a composite electrode of graphite-Teflon-peroxidase-ferrocene; however, the sensor could detect bacteria only when the concentrations reach as high as 2×10^6 CFU/ml [27]. To the best of our knowledge, catalase reaction-based potentiometric sensors for bacterial monitoring are not available [28]. As catalase stands as one of the most efficient enzymes in nature, with turnover rates reaching as high as 2.8 million molecules per second, tests reliant on catalase enzyme activity are inevitably faster [29]. Additionally, all coliforms that serve as indicators for the water quality produce catalase enzymes. The latter's presence in water is a very reliable indicator of bacterial and organic matter contamination [6]. Hence, the sensors that determine the catalase activity in water with precision, can strongly correlate with biological contamination and BOD [30].

The study aims to develop an effective onsite bacterial monitoring tool by integrating electrochemical principles with catalase activity, ensuring rapid and reliable applications. In this study, catalase and catalase-positive bacteria in water are detected using abiotic MnO_2 -coated electrodes when samples are spiked with H_2O_2 . The sensor's response to various concentrations of bacteria and catalase is investigated. Additionally, a thorough review of the sensor's figures of merit, including sensitivity, limit of detection, repeatability, the impact of interfering chemicals, drift, and shelf life, is presented in the paper. Similarly, the sensor's usefulness for real sample tests is experimentally demonstrated.

2. Material and methods

2.1. Reagents and materials

All the reagents used in this study were of analytical grade and deionized (DI) water was used to make the appropriate dilutions. Graphite felt (Nickunj Eximp Ent. Pvt. Ltd, Mumbai), hydrogen peroxide (Fisher Scientific), copper wire (gauge 0.2 mm, Local market), manganese oxide or MnO_2 (Sigma-Aldrich), polytetrafluorethylene or PTFE (Sigma-Aldrich), n-butanol (Fisher Scientific), Luria Bertani (LB) broth (HiMedia), and catalase from bovine liver (C9322, 2000–5000 units/mg protein, Sigma-Aldrich) were procured, and used without further purification. All the measurements were done using an LXI data acquisition unit (34972A, Keysight Technologies), having a 0.004% basic dcV accuracy and ultra-low reading noise (www.keysight.com). Ag/AgCl reference electrode (012167, RE-1B, ALS Co., Ltd., Japan) is used in this study which has a potential (E_0) of 195 mV vs RHE at 25 °C (<https://www.als-japan.com/1388.html>).

2.2. Fabrication of MnO_2 -modified electrodes

Graphite felt (1 cm \times 1 cm) was pre-treated as described previously [31], and termed bare GF. A coating solution consisting of MnO_2 (0.5 M), PTFE (5% v/v), and n-butanol dispersed in DI water, was prepared and homogenized on a magnetic stirrer for 20 min. Next, the pre-treated graphite felts were suspended in the homogenous coating solution and subjected to ultrasonication at 60 °C for 30 min. This was followed by overnight drying of electrodes in a hot air oven at 80 °C. Subsequently, dried electrodes were subjected to heat annealing in a furnace at 360 °C for 60 min. The modified electrodes (termed modified GF) were cooled, and stored in a dark box at room temperature until further use [17,32,33].

2.3. Characterization of electrodes

The cyclic voltammetry (CV) response of bare and modified GF was recorded using a potentiostat (EC-Lab®, Bio-Logic SP-300 electrochemical workstation). The scanning window of the experiment was -1 V to 1 V (vs. Ag/AgCl as reference electrode) and Platinum was used as an inert metal counter electrode at a scanning speed of 10 mV/s. The current responses were recorded by immersing the electrodes in H_2O_2 (0.98 M), phosphate buffer (50 mM) solution, or *E. coli* (2.5×10^8 CFU/ml) in H_2O_2 (0.98 M) separately to measure the performance. A 5 ml of *E. coli* culture in LB media was centrifuged, and collected cell pellets were mixed with 5 ml DI water when used for the CV experiment. The surface area of the modified and bare GFs was determined using Brunauer Emmett

Teller (BET) analysis conducted with Quantachrome instruments. The electrode morphologies were analyzed using a scanning electron microscope (SEM, SEM- EVO 18, Carl Zeiss) equipped with energy-dispersive X-ray spectroscopy (EDS, EDS-51-ADDD-0048, Oxford Instruments). For this study, a bare GF, a modified GF, and a used modified GF (after 100 uses) were observed. These electrodes were subjected to gold sputtering and images were captured at different magnifications and resolutions. The presence of different elements was confirmed using EDS.

2.4. Sensor assembly and its operation

The detection unit contains modified GF (size: 1 cm × 1 cm) as the working electrode (MnO₂-modified graphite electrode), and Ag/AgCl as a reference electrode (Fig. 1). To check the response of MnO₂-modified graphite electrodes, a range of H₂O₂ concentrations were tested, and the response voltage was recorded. The tested concentration range of H₂O₂ is 0.16 M–3.26 M. Briefly, the working and reference electrodes were placed in an amber tube containing 10 ml of H₂O₂ test solution. Both these electrodes were connected to an LXI data acquisition unit, and the response voltage was recorded. The electrodes were rinsed with DI water after each measurement. After calibrating the sensor for H₂O₂ response, subsequent experiments were conducted with 0.98 M H₂O₂, where both working and reference electrodes were placed in an amber tube containing a 10 ml working solution of 1:1 ratio of 0.98 M H₂O₂ and test sample (catalase or bacterial solution).

2.5. Preparation of standard catalase solution and bacterial cultures

A stock solution of catalase was prepared by dissolving one mg of catalase powder from bovine liver, in 10 ml of phosphate buffer (50 mM). The working solutions of catalase were prepared using the stock solution, and diluted appropriately with phosphate buffer (50 mM). The catalase activity in the solution was verified using a method reported previously [34]. Briefly, a catalase solution (100 U/ml) was reacted with 0.036% (w/w) H₂O₂ (each prepared in 50 mM phosphate buffer). The blank reading of 0.036% (w/w) H₂O₂ was measured. A 0.10 ml catalase solution was added into 2.9 ml of 0.036% (w/w) H₂O₂, and OD₂₄₀ was measured using a spectrophotometer. The time taken during the change in OD₂₄₀ from 0.45 to 0.40 was recorded. The final catalase concentration was calculated as described previously, and reported for the further experiments [34].

Three different bacterial strains namely, *E. coli*, *P. aeruginosa*, and *C. youngae* were cultivated in an LB broth or agar as per the standard microbiological procedure. The cultures were cultivated in the broth till the optical density at 600 nm (OD₆₀₀) of 1. The OD₆₀₀ is a measure of bacterial cell density and can be quantified using a spectrophotometer [35]. The serial dilutions of bacterial cultures were prepared in DI water. Colony formation units (CFU) were measured by spread-plating on LB with 1.5% (w/v) agar. The limit of detection (LOD) was calculated using linear regression using Equation (1) as specified previously [36]:

$$\text{Limit of detection (LOD)} = 3.3 \times \sigma / S \quad (1)$$

where σ is the standard deviation of the response, and S is the slope of the calibration curve.

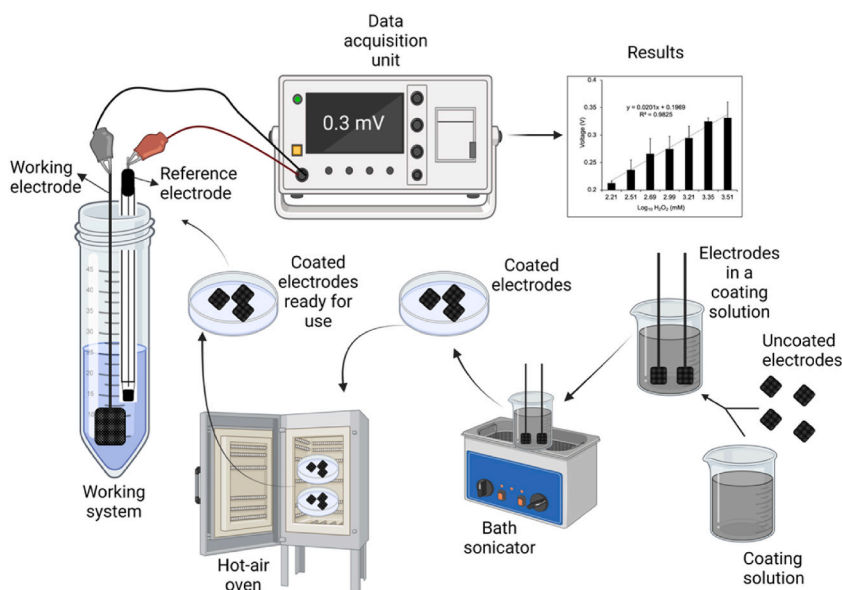


Fig. 1. The schematic shows the sensor fabrication and its working. The sensor fabrication steps involve pre-treatment of graphite felt electrodes, coating of the electrodes, drying of the coated electrodes, and working assembly of the sensor, including working and Ag/AgCl reference electrodes.

2.6. Analytical performance of the sensor

To assess the effect of interfering compounds, different chemical compounds including, ammonium sulphate (400 ppm), sodium nitrate (50 ppm), sodium carbonate (60 ppm), sodium dihydrogen phosphate (100 ppm), glucose (12,000 ppm), and urea (4000 ppm) were tested, as reported by Ramanujam et al. [37]. The test was carried out first by measuring the response of each compound alone, followed by all compounds mixed together. The response voltage was measured for each condition. In each condition, 0.98 M H_2O_2 was mixed with 1 ml of test solution in a 1:1 ratio. Subsequently, a mixed solution was added with two different bacterial concentrations with 0.98 M H_2O_2 in a 1:1 ratio, and response voltage was recorded for both conditions. Control experiments were performed with bacterial cultures (without mixed compounds) having 100 CFU/ml and 10^8 CFU/ml of *E. coli*. First, the bacterial concentrations were mixed with 0.98 M H_2O_2 , and incubated for 5 min, thereafter, the voltage was measured.

To measure the drift in the signals, 100 CFU/ml, 10000 CFU/ml, and 10^8 CFU/ml of *E. coli* culture samples with 0.98 M (1:1 ratio) were tested. DI water was used as a control. About 100 measurements were conducted with the same electrode to test its reusability and reproducibility of signals.

2.7. Application of sensor for real water samples

The real water samples were tested with the sensor to determine the water quality. For this purpose, various water samples were collected that includes DI water (no detectable bacteria), packaged drinking water (different brands), tap water (up to 30 CFU/ml), grey water (sterilized), grey water (6200–6800 CFU/ml). The grey water samples were collected from the inlet of the decentralized wastewater treatment system (DEWATS) at IIT Jodhpur campus. These samples were tested by mixing with 0.98 M H_2O_2 in 1:1 ratio as described in previous sections. Jal TARA water testing kit and HI 3812 hardness test kit (Hanna instruments) were used to characterize different water samples. The recoveries in real samples were tested in semi-continuous monitoring as well to determine the sensor

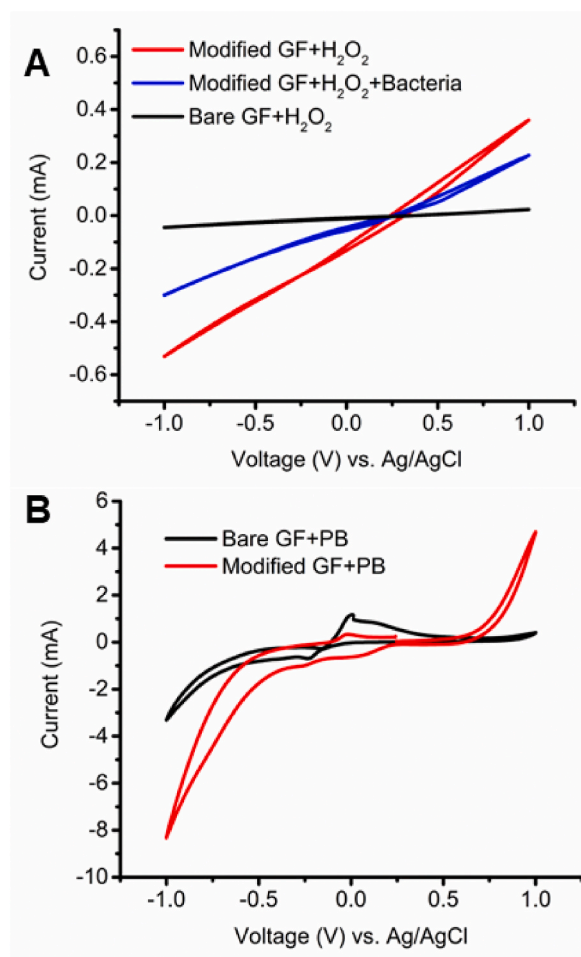


Fig. 2. The CV curves of A) bare and MnO_2 -modified graphite felt (GF) in H_2O_2 solution with/without bacteria, and B) bare and modified GF in phosphate buffer solution. Voltage (V) is measured vs. Ag/AgCl reference electrode.

efficacy. These tests were conducted with the same electrode for 100 min in which electrodes were in continuous contact with water.

2.8. Statistical analysis

All the experiments were performed in triplicates and repeated several times to check the reproducibility ($n = 3$). Regression analysis and sensor linear ranges were determined using Microsoft Excel. 2-way ANOVA test was used to analyze the three data sets using the software GraphPad Prism 8.0.1.

3. Results and discussion

3.1. Effect of MnO_2 coating on electrode response

The electrocatalytic performance of electrodes was evaluated by comparing the voltammetric behaviour through the CV. The capacitive background current increased with MnO_2 modification of GF electrodes, as compared with bare GF electrodes, as shown in Fig. 2A and B in H_2O_2 (0.98 M) and phosphate buffer (PB) solution, respectively. The modified electrode has an increased surface area of $55.65 \text{ m}^2/\text{g}$ and a larger pore area compared to the original GF surface area of $25.99 \text{ m}^2/\text{g}$. The increased surface area of the modified GF results in a 58.74% prevalence of O_2 -rich surface, resulting in a decrease in the potential difference between peaks and significant enhancements in the current at the peaks. Moreover, the metal oxides can undergo redox reactions on the electrode interface resulting in anodic and cathodic currents. Bare GF, on the other hand, does not have any redox active compounds that display signals upon CV analysis. This CV trend obtained in the present study has similarities with profiles reported earlier in PB solution [38, 39]. Redox peaks were absent in the CV of modified electrodes acquired in H_2O_2 solution prepared in DI water which is expected as the solution has no conductivity. The results indicate that MnO_2 increases the electroactivity of the electrodes which results in the high rate of electron transfer [40] (Fig. 2A). H_2O_2 causes disturbances in the cell structure and permeability of the cell wall and membrane, thereby lysing the cells which further allow the cell constituents to be released from the cell. Adding the H_2O_2 to the bacterial solution causes the breakdown of the H_2O_2 in H_2O and O_2 [41]. Both are non-conductive species; hence, no redox peaks were observed. The consumption of H_2O_2 in the presence of bacteria leads to decrease in the current produced as compared to fresh H_2O_2 solution as shown in Fig. 2A. This indicates that the sensor is suitable for an amperometric response as well.

A very similar trend was also reported previously, where electrochemical measurement of H_2O_2 was investigated using catalase enzyme-coated on NAF/MWCNTs electrodes [10]. In the later study, when CV was performed in PB or H_2O_2 solution without bacteria,

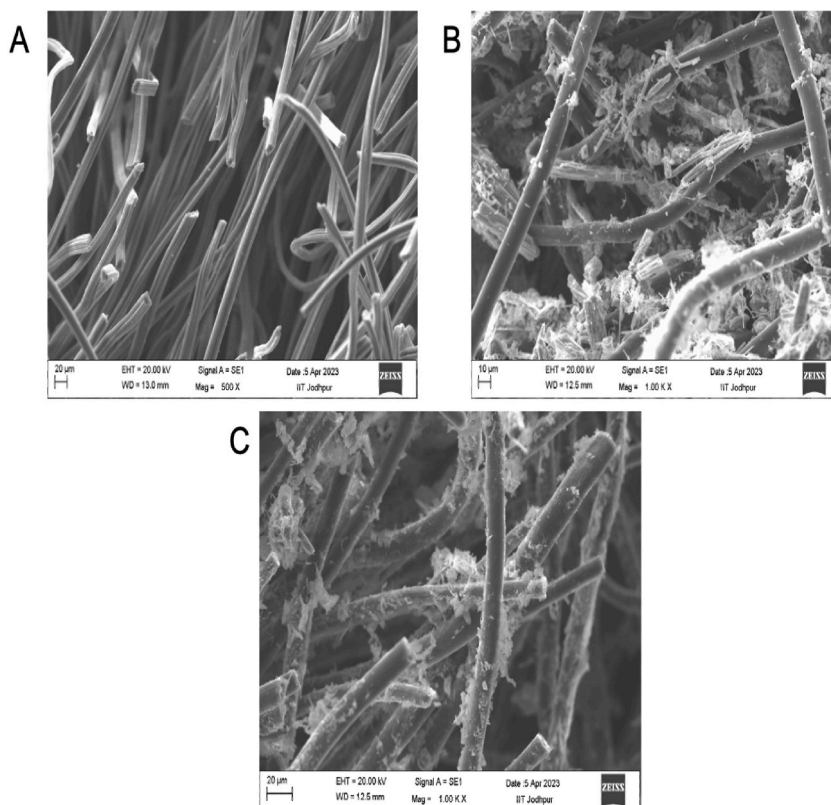


Fig. 3. SEM images of A) bare Graphite Felt (GF), B) fresh MnO_2 -modified GF, and C) used MnO_2 -modified GF (used up to 100 times).

no significant peaks were observed at the electrode interface. The number of cycles can be varied for more detailed CV analysis of these modified electrodes. However, the present study is more focused on identifying the differences between bare and MnO₂ modified electrodes.

3.2. SEM and EDS analysis of the working electrodes

Fig. 3 shows the morphology of the bare graphite felt and MnO₂-modified graphite felt, respectively. The modified electrode exhibited altered morphology with a rough surface over the bare electrode. The SEM images of the used electrode are also showing the altered morphology which suggest the stability of MnO₂ coating after repeated use. The EDS shows (Fig. 4) the representative peaks for Mn, C, and O in modified electrodes. The Mn peak was absent in bare graphite felt. The free electrons in graphite felt may form the π -bond with the MnO₂ particles allowing a stably modified electrode [42]. The results were in line with studies reported previously [32]. The Mn peak intensity dropped in the used electrode (after 100 tests) indicating withering of Mn.

3.3. Potentiometric response of the sensor with pure catalase and bacteria

The working electrode potential (vs. Ag/AgCl electrode) increases linearly with increasing H₂O₂ concentrations. The H₂O₂ interacts with MnO₂ groups causing its cyclic oxidation/reduction on electrode interface. Previous studies have also shown the calibration curve for modified electrodes, which shows linear response in the range of 3.00×10^{-7} – 3.63×10^{-4} M H₂O₂ where rise in the potential can be observed [24]. However, when catalase or catalase-positive bacteria are introduced into the solution, they decompose H₂O₂ to H₂O and O₂, leading to a notable reduction in the electrode potential. This serves as the basis to measure bacterial/catalase activity in water. The decomposition of H₂O₂ was studied by measuring the reduction potential of the working electrode against the Ag/AgCl reference electrode. The electrode potential was plotted as a function of Log₁₀H₂O₂ as shown in Fig. 5A to obtain a calibration curve. The calibration equation obtained in the given experimental conditions is $y = 0.0909x + 0.0114$, where y is the voltage in volts (vs. Ag/AgCl) and x is the Log₁₀C (H₂O₂ concentration, mM). The response of modified GF towards H₂O₂ paved the path to explore it as a potentiometric catalase sensor.

The calibration curve for catalase activity and bacterial concentrations were prepared by first mixing the catalase or bacterial dilution with 0.98 M H₂O₂ in 1:1 ratio and incubating for 5 min. The electrodes (working and reference) are then immersed in the solution to measure the electrode potential. The results are represented in Fig. 5 where the curves are plotted with the best fitted points.

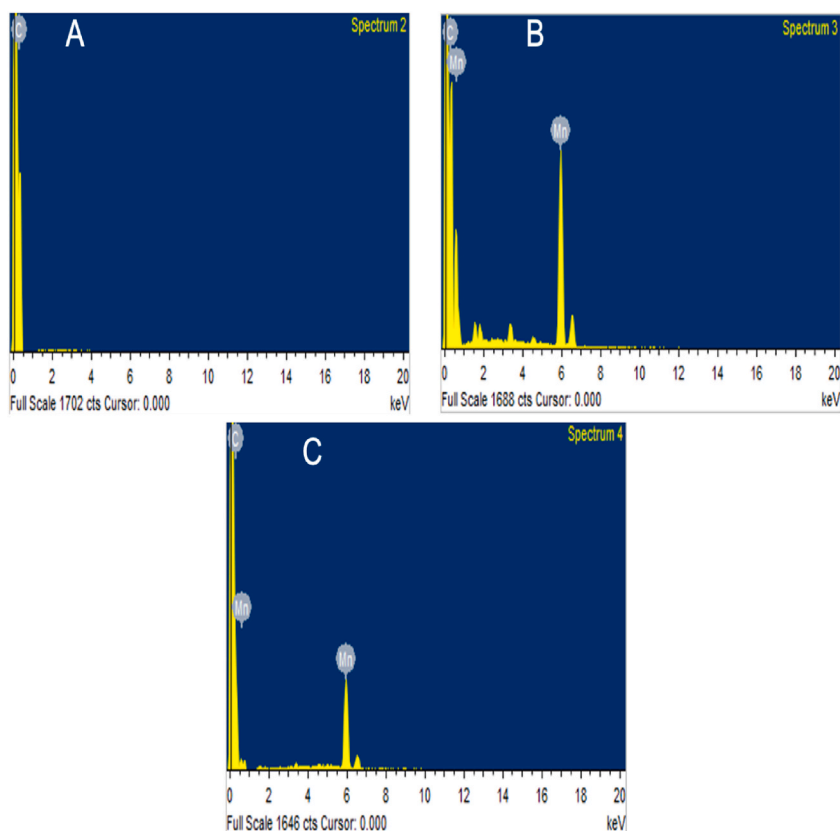


Fig. 4. EDS spectra of A) bare Graphite Felt (GF), B) fresh MnO₂-modified GF, and C) used MnO₂-modified GF (used up to 100 times).

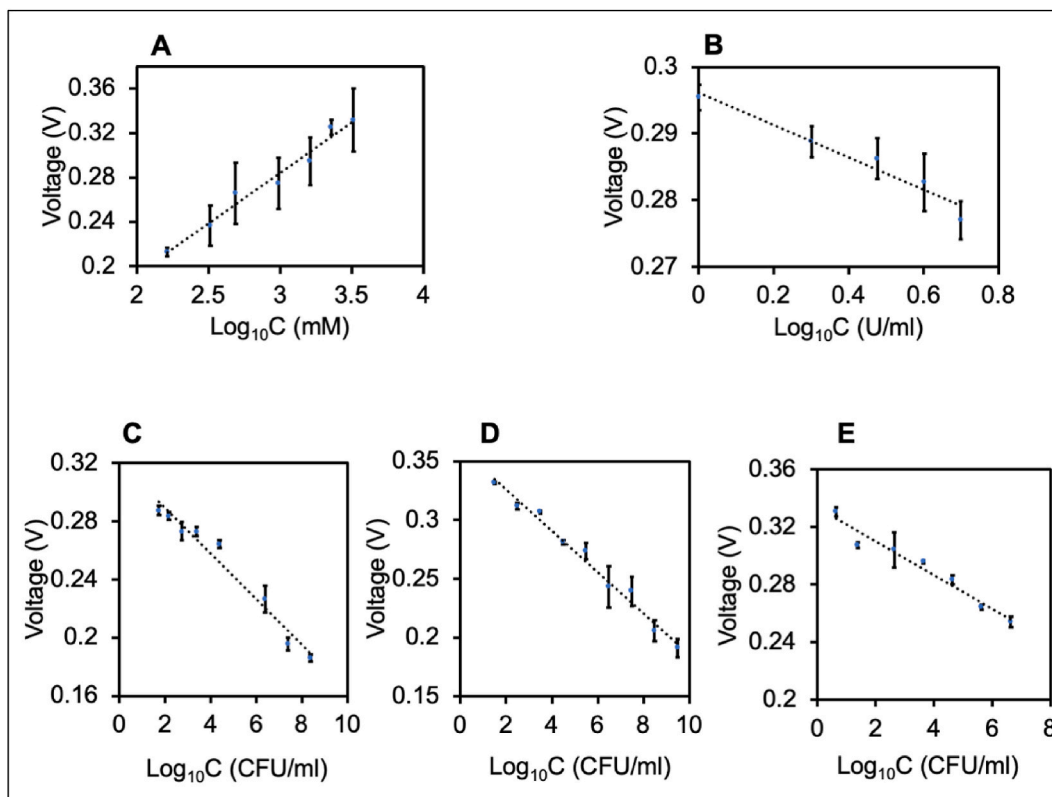


Fig. 5. The sensor response curves for A) H_2O_2 : voltage vs. Log_{10}C (mM) $y = 0.0909x + 0.0114$, B) Catalase: voltage vs. Log_{10}C (U/ml), $y = -0.0243x + 0.2961$, C-E) voltage vs. Log_{10}C (CFU/ml) for *E. coli* ($y = -0.0157 + 0.3208$), *P. aeruginosa* ($y = -0.0175x + 0.3612$) and *C. youngae* ($y = -0.0117x + 0.3334$), respectively.

Table 1

Comparison of existing sensors for catalase-positive bacteria.

S. No.	Target organism	Limit of detection (CFU/ml)	Linear range of detection (CFU/ml)	Assay time	Detection mechanism	References
1	<i>P. aeruginosa</i>	20	–	50 min	Lateral flow nucleic acid biosensor	[2]
2	<i>E. coli</i>	10	10^6 – 10^8	60 min	H_2O_2 -selective organic/inorganic-hybrid sol-gel film-(Pt) electrode.	[25]
3	<i>E. coli</i>	<100	100 – 10×10^5	<10 min	Lateral flow immunoassay-based amperometric sensor	[26]
4	<i>E. coli</i>	11640	1×10^6 – 1×10^8	10 min	Nickel based rotating disc electrode	[37]
5	<i>P. aeruginosa</i>		5 to 50	14 s	Electrochemical measurement using biomarker pyocyanin	[47]
6	<i>E. coli</i>	1000	1000 to 1.0×10^9	Within 60 min	Electrochemical method based on p-benzoquinone as a redox mediator to monitor the bacterial concentration	[48]
7	<i>E. coli</i> , <i>P. putida</i> , <i>S. epidermidis</i>	20	20 – 10^5	10 min	Nanostructured Gold/Graphene Microfluidic Device	[49]
8	<i>P. aeruginosa</i>	50		150 s	Polymeric nanofilm is imprinted on the SPR sensor surface with the microcontact printing method	[47]
9	<i>P. aeruginosa</i>	8	10 to 10^5	–	Ferrocene-labelled anti- <i>Ps</i> as redox probe with zeolitic imidazolate framework/gold nano-particle composite as a platform	[50]
10	<i>E. coli</i>	11	54.95 – 1.08×10^6	5 min	MnO_2 modified graphite felt	Present study
11	<i>P. aeruginosa</i>	23	30.73 – 2.97×10^7	5 min	MnO_2 modified graphite felt	Present study
12	<i>C. youngae</i>	12	24.66 – 4.37×10^7	5 min	MnO_2 modified graphite felt	Present study

When the catalase or bacterial concentration increases, the electrode potential vs. Ag/AgCl decreases linearly due to the breakdown of H_2O_2 by the action of catalase. Literature studies have suggested that sensors that respond rapidly to a change of 1 U/ml catalase activity can be very useful for water monitoring [43]. The sensor showed a lower limit of detection (LOD) of 11 CFU/ml for *E. coli*, 12 CFU/ml for *C. youngae*, and 23 CFU/ml for *P. aeruginosa*. The linear detection range for catalase, *E. coli*, *C. youngae*, and *P. aeruginosa* are 0.8–3.40 U/ml, $54.95\text{--}1.08 \times 10^6$ CFU/ml, $24.66\text{--}4.37 \times 10^7$ CFU/ml, and $30.73\text{--}2.97 \times 10^7$ CFU/ml, respectively as shown in Fig. 5B–E. These findings have suggested better LODs than the previous reports based on electrochemical sensors. The linearity range was different for the different bacterial strains which may stem from the metabolic status and intracellular catalase activities of different bacterial species [43].

The sensor offered baseline voltage from 0.30 to 0.34 V in the DI water as control. The sensitivity of the working electrode was high, with a value of 4.83, 3.49, 3.02, and 4.24 mV/cm^2dec for catalase enzymes, *E. coli*, *C. youngae*, and *P. aeruginosa*, respectively. The coefficient of determination (R^2) for regression slopes were 0.99, 0.99, 0.99, and 0.99 for catalase enzymes, *E. coli*, *P. aeruginosa*, and *C. youngae*, respectively. The control experiments consisted of purified catalase enzymes as the positive control while DI water with no detectable bacteria was the negative control. Lower response time, lower LOD, and higher sensitivity of the sensor make it superior to the previously reported sensors [2,27,44,45]. Moreover, the abiotic platforms as used in our study, have higher shelf life and stability over biotic sensors.

The electrochemical measurement of H_2O_2 was previously reported using a Nickel oxidation reaction on a rotating disc electrode showing high specificity for *E. coli* [37]. The lower LOD value was 11640 CFU/ml, which is higher considering the requirement of sensitive bacterial detection in water. A recent study has shown the detection of viable bacterial cells using an amperometric sensor with an indium tin oxide electrode. This sensor had a lower LOD of 28 CFU/ml for *E. coli* with a response time of >60 min [46], while the sensor reported in the current study has a much lower detection value and lower response time. Table 1 summarizes the advantages of the sensor developed in this study with similar studies in the literature. The sensor cannot precisely detect a particular bacterial species, although that can be possible when multiple samples with a mixture of bacteria and individual bacteria are analyzed. The

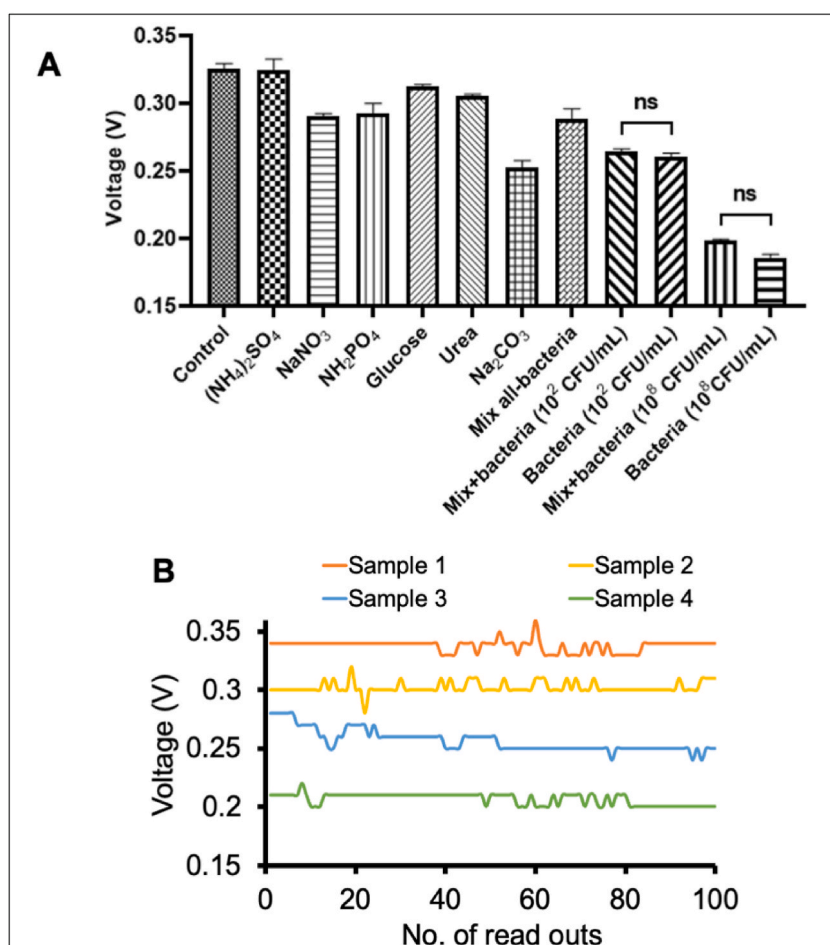


Fig. 6. Graphical representation of A) the effect of interfering substances on sensor response (The interference in the sensor is tested for bacteria with/without mixed interfering solution. Here, ns means no significant change). B) The drift in sensor response after multiple uses (Samples 1: DI water, Sample 2: 100 CFU/ml, Sample 3: 10000 CFU/ml, and Sample 4: 10^8 CFU/ml).

algorithmic analysis of voltage v/s time curves may predict the specific bacteria or combination of bacteria. The catalase activity in bacteria is guided by its physiological status and stress response. Nevertheless, the catalase activities are found in fixed ranges, and it is not difficult to develop a bacterial monitoring device using a sensor developed in our study.

Moreover, the sensor hysteresis can result in different output values for the same input depending on whether the input is increasing or decreasing. To mitigate the effects of hysteresis, calibration techniques and compensation algorithms may be employed to improve the accuracy and reliability of the sensor's measurements. The hysteresis of the developed sensor was assessed, given its reliance on biological components reacting with H₂O₂. Ensuring the vitality of bacteria in the water sample and the stability of H₂O₂ are crucial phenomena for each measurement. In this study, the impact of varying environmental conditions on sensor performance was evaluated, revealing minor fluctuations in the potential of the H₂O₂ solution. The baseline voltage in the absence of bacteria was calibrated within the range of 0.30–0.34 V.

3.4. Sensor selectivity and response time

The possible interfering chemical compounds were tested on the sensor. The compounds tested were ammonium sulphate (400 ppm), sodium nitrate (50 ppm), sodium carbonate (60 ppm), sodium dihydrogen phosphate (100 ppm), glucose (12,000 ppm), and urea (4000 ppm). The results indicated that the test has no interference from urea, ammonium, sulphate, phosphates, and glucose. The carbonate and nitrate slightly triggered the sensor response, as evident by the change in the initial voltage value in the absence of bacteria, indicating them as interfering substances. The presence of carbonate and nitrates triggers the breakdown of H₂O₂ resulting in the lower reduction potential of the solution [51,52]. The sensor signal was relatively stable in the mixture of the said compounds (Fig. 6A), and no significant changes were observed when interfering ions were present along with the bacteria (two-way ANOVA, P-value >0.05). The results followed the previous study by Ramanujam et al. [37]. The sensor stability in the presence of interfering compounds indicated its usefulness for real bacterial monitoring. In addition, the sensor was able to respond in seconds when different bacterial concentrations were introduced in the sensing unit which suggests the applicability of the sensor as a rapid bacterial detection system.

In the absence of bacteria, the potential of H₂O₂ is directly measured. However, for bacterial measurement, a brief incubation period is essential to facilitate interaction between bacteria and H₂O₂. Therefore, the total test duration is 5 min, including the sample mixing and incubation time. Despite the sensor's rapid response within seconds, omitting the required incubation period may lead to erroneous results in case of bacterial monitoring.

3.5. Sensor drift measurement

The sensor was characterized in terms of response time, reproducibility, accuracy, and reusability. The sensor was reused up to 100 times for four samples with different bacterial concentrations (Fig. 6B). Sample 1 is control (DI water), sample 2 is *E. coli* at 100 CFU/ml, sample 3 is *E. coli* at 10000 CFU/ml, and sample 4 is *E. coli* at 10⁸ CFU/ml. For samples 1 to 4, the mean ± SD voltage values are 0.3370 ± 0.005 V, 0.3018 ± 0.005 V, 0.2565 ± 0.009 V, and 0.2065 ± 0.005 V with a coefficient of variation of 1–3%. These results suggested that the sensor signal was stable after repeated use, indicating a low drift (Fig. 6B). A slight rinse with DI water was sufficient to condition the working electrode for subsequent use.

3.6. Sensor application for drinking water and grey water monitoring

The present study has assessed the suitability of the developed sensor for real-time application for monitoring bacterial contamination in drinking and grey water. It was observed that the packaged drinking water samples (two different brands tested) produced signals (0.293 ± 0.014 V) comparable to DI control, indicating that the water samples had no bacteria and interfering compounds. The tap water (bacterial content up to 30 CFU/ml) causes a potential drop in the range of 0.25–0.26 V, while grey water (6200–6800 CFU/ml) shows a higher decline (0.199 ± 0.005 V) indicating a proportionality in the sensor signal and bacterial concentration in water (Table 2). The sterilized tap water and grey water also exhibited a drop in voltage signal due to the presence of nitrate (up to 10 ppm) and carbonates (78–111 ppm). The potential reduction in the unsterilized sample was more significant. These results follow our study with simulated wastewater where nitrates (50 ppm) and carbonates (60 ppm) turned out to be interfering compounds. This indicates that the calibration of the sensor shall be necessary for bacterial monitoring when testing different water samples at various locations, which may have variable concentrations of interfering ions. Nevertheless, the developed sensor works well for water monitoring by

Table 2

The sensor performance for monitoring drinking water and grey water.

S. No.	Sample/Parameters	DI water	Packaged drinking water	Tap water	Grey water (sterilized)	Grey water (unsterilized)
1	pH	7.01 ± 0.06	6.45 ± 0.06	7.59 ± 0.03	7.306 ± 0.035	7.221 ± 0.028
2	Conductivity (µS)	2.43 ± 0.03	182 ± 0.035	295.33 ± 7.57	699 ± 7.93	704 ± 10.58
3	Nitrate (ppm)	–	<10	<10	10	10
4	Carbonate (ppm)	–	45 ± 4.24	84 ± 8.48	103.2 ± 3.12	111 ± 4.24
5	CFU/ml	–	–	0–30	–	6.2 × 10 ³ –6.8 × 10 ³
6	Sensor signal (Voltage, V)	0.323 ± 0.018	0.293 ± 0.014	0.249 ± 0.016	0.221 ± 0.005	0.199 ± 0.001

effectively measuring the drop in the reduction potential of the solution in the presence of bacterial contamination. These results support the usefulness of the sensor for real-time measurements.

3.7. Sensor cost analysis

The developed sensor was compared with the existing bacterial sensors and a cost analysis is presented in this section. The developed system costs approximately 350 INR or 4.53 USD per unit which is relatively lower over the existing biosensors/biotic sensor electrodes. The development of the sensor system involves the design of interface circuits, read-out electronics, embedded algorithms for drift compensation and signal conditioning, analog to digital converter and LCD display. The complete sensor system is expected to cost 12–18 USD which is relatively less considering its figures of merit. The available bacterial meters, namely ATP Meters & Swabs costs £150.00 – £1671.01. These detect water contaminants, including food contaminants, allergens, and bacteria. In addition, the Bactaslyde *E. coli* test kit costs 13.85 USD per test. Recently developed PadmaBio *E. coli* testing box costs 2.40 USD per test; however, the test requires 24 h test time (<https://www.earthface.in/product/padma-bio>). These studies suggest cost-effective bacterial monitoring in water.

3.8. Performance and the possible mechanism of the sensor

The mechanism of MnO₂-modified carbon electrodes for H₂O₂ detection has been explained previously [24,25]. Briefly, MnO₂ oxidizes and forms MnO₄²⁻ or Mn₂O₃ increasing the potential developed at the sensor interface. With the increased concentration of H₂O₂, the electrode potential increases. In the presence of catalase/bacteria, the H₂O₂ concentration decreases, resulting in a low electrode potential. The sensor eventually regenerates itself through the reverse reaction of MnO₄²⁻ or Mn₂O₃ to MnO₂. Both the electrode and coating material are quite stable at ambient conditions and do not require specific storage conditions [53]. When the sensor was employed for semi-continuous water monitoring, it regenerates its surface and reaches the same initial potential reading after taking measurements in real samples indicating good recovery. The sensor surface could show stability up to 60 min only when it was continuously immersed in water. After 60 min, the sensor response was unstable which might be due to removal of MnO₂ coating.

3.9. Challenges and the way forward

The present study has addressed several technical challenges associated with coliform sensing that includes the use of a cost-effective electrode with an increased detection range for catalase-positive bacteria. The modified electrode is responsive to H₂O₂ in a linear range of 0.16 M–3.26 M, which is suitable for measuring catalase activity. The study has shown the higher sensitivity of the working electrodes than the prior art, with an improved response time. Previous studies with MnO₂-modified electrodes have not shown bacterial monitoring. This suggests that the modified electrode can detect coliforms more quickly and accurately than the previous methods [37,48]. The use of an abiotic sensing system improves the shelf life and storage of the system. However, a continuous supply of H₂O₂ solution is needed. The H₂O₂ is light-sensitive and needs to be stored in the dark. The appropriate initial concentration of H₂O₂ is critical for sensor response. This aspect needs future work to determine the constant supply and concentration of H₂O₂ for consistent results. The electrodes used in the present work are easy to prepare, scalable, and can be easily operated with minimum technical knowledge which may make coliform sensing methods more accessible and practical for a wider range of users. These sensor mechanisms can be adapted on paper substrates for miniaturization or lateral flow assays to enhance the ease of operation of the sensor [54].

This study examined the impact of ions on sensor performance, revealing negligible to minimal interference. Furthermore, the sensor's efficacy was assessed using real water samples, reinforcing its suitability for bacterial monitoring applications. In regions characterized by elevated concentrations of water contaminants, pre-filtration can be implemented to mitigate potential effects on sensor performance. While previous studies have advocated bacterial enrichment or separation, such procedures introduce testing delays and impede the practical onsite application of the developed sensor by necessitating bacterial separation from the water sample. Therefore, the present sensor has been designed with the objective of enabling cost-effective bacterial detection in remote locations, eliminating the reliance on laboratory environments. Also, the present study utilizes H₂O₂ as the test reagent, which also undergoes spontaneous decomposition. Therefore, the measurements were done in batch mode. However, if the complete device is constructed with this sensor, allowing for semi-continuous measurements, it becomes feasible to perform such continuous monitoring directly from water channels.

4. Conclusions

This study has investigated the suitability of MnO₂-modified carbon electrodes for rapid potentiometric detection of catalase/catalase-positive bacteria with a lower limit of detection of 11–23 CFU/ml. The method doesn't require any pre-enrichment or concentration step. The sensor is deployable in low-resource settings. The developed sensor offers long shelf life, good linearity of the signals with various concentrations of catalase/catalase-positive bacteria, and minimal interference from other water contaminants. The sensor response to drinking water as well as wastewater makes it promising for real-time applications. The design of interface circuits with embedded drift compensation algorithms and read-out circuits for LCDs will constitute future studies on miniaturized chip-based electrodes.

CRediT authorship contribution statement

Arti Sharma: Writing – review & editing, Writing – original draft, Visualization, Validation, Software, Project administration, Methodology, Investigation, Formal analysis, Data curation, Conceptualization. **Akanksha Mishra:** Writing – review & editing, Writing – original draft, Visualization, Validation, Software, Project administration, Methodology, Investigation, Formal analysis, Data curation, Conceptualization. **Meenu Chhabra:** Writing – review & editing, Writing – original draft, Visualization, Validation, Supervision, Software, Resources, Project administration, Methodology, Investigation, Funding acquisition, Formal analysis, Conceptualization.

Declaration of competing interest

The authors declare that they have no known competing financial interests or personal relationships that could have appeared to influence the work reported in this paper.

Acknowledgments

The project was supported by Jal Jeevan Mission, Department of Drinking Water and Sanitation, Ministry of Jal Shakti, Government Of India (W-11042/19/2022-JJM-IV-DDWS). Authors AS and AM would like to thank the DST-INSPIRE Fellowship (IF190164) and the Ministry of Education, India, respectively for supporting their Ph.D. work.

References

- [1] American Public Health Association, American water works association, water pollution control federation, water environment federation, in: *Standard Methods for the Examination of Water and Sewage* (2), American Public Health Association, 1912.
- [2] Y. Chen, N. Cheng, Y. Xu, K. Huang, Y. Luo, W. Xu, Point-of-care and visual detection of *P. aeruginosa* and its toxin genes by multiple LAMP and lateral flow nucleic acid biosensor, *Biosens. Bioelectron.* 81 (2016) 317–323, <https://doi.org/10.1016/j.bios.2016.03.006>.
- [3] K.G. Kerr, A.M. Snelling, *Pseudomonas aeruginosa*: a formidable and ever-present adversary, *J. Hosp. Infect.* 73 (2009) 338–344, <https://doi.org/10.1016/j.jhin.2009.04.020>.
- [4] X. Zhang, L. Chen, Z. Shen, Impacts of rapid urbanization on characteristics, sources and variation of fecal coliform at watershed scale, *J. Environ. Manag.* 286 (2021) 112195, <https://doi.org/10.1016/j.jenvman.2021.112195>.
- [5] B.B. Hosetti, S. Frost, Catalase activity in wastewater, *Water Res.* 28 (1994) 497–500, [https://doi.org/10.1016/0043-1354\(94\)90289-5](https://doi.org/10.1016/0043-1354(94)90289-5).
- [6] L.F. Pedersen, P. Rojas-Tirado, E. Arvin, P.B. Pedersen, Assessment of microbial activity in water based on hydrogen peroxide decomposition rates, *Aquacult. Eng.* 85 (2019) 9–14, <https://doi.org/10.1016/j.aquaeng.2019.01.001>.
- [7] P.B. Duke, J.D. Jarvis, The catalase test—a cautionary tale, *Med. Lab. Technol.* 29 (1972) 203–204.
- [8] T. Iwase, A. Tajima, S. Sugimoto, K.I. Okuda, I. Hironaka, Y. Kamata, Y. Mizunoe, A simple assay for measuring catalase activity: a visual approach, *Sci. Rep.* 3 (2013) 3081, <https://doi.org/10.1038/srep03081>.
- [9] L. Aghebati-maleki, B. Salehi, R. Behfar, H. Saeidmanesh, F. Ahmadian, M. Sarebanhassanabadi, M. Negahdary, Designing a hydrogen peroxide biosensor using catalase and modified electrode with magnesium oxide nanoparticles, *Int. J. Electrochem. Sci.* 9 (2014) 257–271, [https://doi.org/10.1016/S1452-3981\(23\)07714-3](https://doi.org/10.1016/S1452-3981(23)07714-3).
- [10] G. Fusco, P. Bollella, F. Mazzei, G. Favero, R. Antiochia, C. Tortolini, Catalase-based modified graphite electrode for hydrogen peroxide detection in different beverages, *J. Anal. Methods Chem.* (2016), <https://doi.org/10.1155/2016/8174913>.
- [11] D. Soto, M. Alzate, J. Gallego, J. Orozco, Hybrid nanomaterial/catalase-modified electrode for hydrogen peroxide sensing, *J. Electroanal. Chem.* 880 (2021) 114826, <https://doi.org/10.1016/j.jelechem.2020.114826>.
- [12] M. Dinesh, C. Revathi, Y. Haldorai, R.T.R. Kumar, Birnessite MnO₂ decorated MWNTs composite as a nonenzymatic hydrogen peroxide sensor, *Chem. Phys. Lett.* 731 (2019) 136612, <https://doi.org/10.1016/j.cplett.2019.136612>.
- [13] S. Momeni, R. Ahmadi, F. Farjami, Nonenzymatic electrochemical assay for hydrogen peroxide detection based on green synthesized MnO₂ nanosheets, *Mater. Res. Express* 6 (2020) 1250f6, <https://doi.org/10.1088/2053-1591/ab65e2>.
- [14] Y. Shu, J. Xu, J. Chen, Q. Xu, X. Xiao, D. Jin, X. Hu, Ultrasensitive electrochemical detection of H₂O₂ in living cells based on ultrathin MnO₂ nanosheets, *Sensor. Actuator. B Chem.* 252 (2017) 72–78, <https://doi.org/10.1016/j.snb.2017.05.124>.
- [15] B. Xu, M.L. Ye, Y.X. Yu, W.D. Zhang, A highly sensitive hydrogen peroxide amperometric sensor based on MnO₂-modified vertically aligned multiwalled carbon nanotubes, *Anal. Chim. Acta* 674 (2010) 20–26, <https://doi.org/10.1016/j.aca.2010.06.004>.
- [16] L.F. Castañeda, F.C. Walsh, J.L. Nava, C.P. de Leon, Graphite felt as a versatile electrode material: properties, reaction environment, performance and applications, *Electrochim. Acta* 258 (2017) 1115–1139, <https://doi.org/10.1016/j.electacta.2017.11.165>.
- [17] E. Mehmeti, D.M. Stanković, S. Chaiyo, L. Švorc, K. Kalcher, Manganese dioxide-modified carbon paste electrode for voltammetric determination of riboflavin, *Microchim. Acta* 183 (2016) 1619–1624, <https://doi.org/10.1007/s00604-016-1789-4>.
- [18] F.A. Abdel-Aal, A.H. Rageh, M.I. Said, G.A. Saleh, ε-MnO₂-modified graphite electrode as a novel electrochemical sensor for the ultrasensitive detection of the newly FDA approved Hepatitis C antiviral drug ledipasvir, *Anal. Chim. Acta* 1038 (2018) 29–40, <https://doi.org/10.1016/j.aca.2018.07.018>.
- [19] H. Cheng, J. Liu, Y. Sun, T. Zhou, Q. Yang, S. Zhang, W. Sun, A fungus-derived biomass porous carbon–MnO₂ nanocomposite-modified electrode for the voltammetric determination of rutin, *RSC Adv.* 10 (2020) 42340–42348, <https://doi.org/10.1039/D0RA05739H>.
- [20] Y. Wang, Y. Liu, I. Zhitomirsky, Surface modification of MnO₂ and carbon nanotubes using organic dyes for nanotechnology of electrochemical supercapacitors, *J. Mater. Chem. A* 1 (2013) 12519–12526, <https://doi.org/10.1039/c3ta12458d>.
- [21] C.S. Pundir, R. Deswal, V. Narwal, Quantitative analysis of hydrogen peroxide with special emphasis on biosensors, *Bioproc. Biosyst. Eng.* 41 (2018) 313–329, <https://doi.org/10.1007/s00449-017-1878-8>.
- [22] S.H. Do, B. Batchelor, H.K. Lee, S.H. Kong, Hydrogen peroxide decomposition on manganese oxide (pyrolusite): kinetics, intermediates, and mechanism, *Chemosphere* 75 (2009) 8–12, <https://doi.org/10.1016/j.chemosphere.2008.11.075>.
- [23] A.B. Hart, J. McFadyen, R.A. Ross, Solid-oxide-catalyzed decomposition of hydrogen peroxide vapour, *Trans. Faraday Soc.* 59 (1963) 1458–1469.
- [24] X. Zheng, Z. Guo, Potentiometric determination of hydrogen peroxide at MnO₂-doped carbon paste electrode, *Talanta* 50 (2000) 1157–1162, [https://doi.org/10.1016/S0039-9140\(99\)00223-4](https://doi.org/10.1016/S0039-9140(99)00223-4).
- [25] R. Wang, Y. Shi, H. Wang, J. Yang, J. Zhu, Y. Chen, N. Yuan, Electrochemical study of hydrogen peroxide detection on MnO₂ micromaterials, *Int. J. Electrochem. Sci.* 11 (2016) 5962–5972, <https://doi.org/10.20964/2016.07.42>.
- [26] Y. Hasebe, M. Fukuzawa, H. Matsuhisa, Quantitative determination of *Escherichia coli* based on the electrochemical measurement of bacterial catalase activity using H₂O₂-selective organic/inorganic-hybrid sol-gel film-modified Pt electrode, *J. Environ. Sci.* 21 (2009) S44–S47, [https://doi.org/10.1016/S1001-0742\(09\)60034-6](https://doi.org/10.1016/S1001-0742(09)60034-6).

- [27] B. Serra, J. Zhang, M.D. Morales, A.G.V. de Prada, A.J. Reviejo, J.M. Pingarron, A rapid method for detection of catalase-positive and catalase-negative bacteria based on monitoring of hydrogen peroxide evolution at a composite peroxidase biosensor, *Talanta* 75 (2008) 1134–1139, <https://doi.org/10.1016/j.talanta.2008.01.009>.
- [28] D. Kadadou, L. Tizani, V.S. Wadi, F. Banat, H. Alsafar, A.F. Yousef, S.W. Hasan, Recent advances in the biosensors application for the detection of bacteria and viruses in wastewater, *J. Environ. Chem. Eng.* 10 (2022) 107070, <https://doi.org/10.1016/j.jece.2021.107070>.
- [29] A.N. Eremin, I.V. Moroz, R.V. Mikhailova, Use of cadmium hydroxide gel for isolation of extracellular catalases from *Penicillium piceum* and characterization of purified enzymes, *Appl. Biochem. Microbiol.* 44 (2008) 590–599, <https://doi.org/10.1134/S0003683808060069>.
- [30] A. Ardila, M.J. Rodriguez, G. Pelletier, Spatiotemporal optimization of water quality degradation monitoring in water distribution systems supplied by surface sources: a chronological and critical review, *J. Environ. Manag.* 337 (2023) 117734, <https://doi.org/10.1016/j.jenvman.2023.117734>.
- [31] A. Sharma, M. Chhabra, Performance evaluation of a photosynthetic microbial fuel cell (PMFC) using *Chlamydomonas reinhardtii* at cathode, *Bioresour. Technol.* 338 (2021) 125499, <https://doi.org/10.1016/j.biortech.2021.125499>.
- [32] Y. Qiu, X. Zhang, S. Yang, High performance supercapacitors based on highly conductive nitrogen-doped graphene sheets, *Phys. Chem. Chem. Phys.* 13 (2011) 12554–12558, <https://doi.org/10.1039/C1CP21148J>.
- [33] Y. Qiu, P. Xu, B. Guo, Z. Cheng, H. Fan, M. Yang, J. Li, Electrodeposition of manganese dioxide film on activated carbon paper and its application in supercapacitors with high rate capability, *RSC Adv.* 4 (2014) 64187–64192.
- [34] R.F. Beers, I.W. Sizer, A spectrophotometric method for measuring the breakdown of hydrogen peroxide by catalase, *J. Biol. Chem.* 195 (1952) 133–140.
- [35] J. Beal, N.G. Farny, T. Haddock-Angelli, V. Selvarajah, G.S. Baldwin, R. Buckley-Taylor, iGEM Interlab Study Contributors, Robust estimation of bacterial cell count from optical density, *Commun. Biol.* 3 (2020) 512, <https://doi.org/10.1038/s42003-020-01127-5>.
- [36] I.H.T. Guideline, Validation of analytical procedures: text and methodology, *Q2 1 (R1)* (2005) 5.
- [37] A. Ramanujam, B. Neyhouse, R.A. Keogh, M. Muthuvel, R.K. Carroll, G.G. Botte, Rapid electrochemical detection of *Escherichia coli* using nickel oxidation reaction on a rotating disk electrode, *J. Chem. Eng.* 411 (2021) 128453, <https://doi.org/10.1016/j.ccej.2021.128453>.
- [38] J.B. Raoof, R. Ojani, F. Chekin, Electrochemical oxidation of 4-chlorocatechol in the presence of some sulphhydryl compounds: applications to voltammetric detection of D-penicillamine, glutathione and L-cysteine, *Anal. Bioanal. Electrochem.* 1 (2009) 200–215.
- [39] S.B. Tanuja, B.K. Swamy, K.V. Pai, Cyclosporine/SDS modified carbon paste electrode for electrochemical study of dopamine: a cyclic voltammetric study, *J. Electroanal. Chem.* 2 (2016) 2–8, <https://doi.org/10.21767/2470-9867.100016>.
- [40] V.S. Haritha, A. Vijayan, S.S. Kumar, R.B. Rakhi, Voltammetric determination of hydrogen peroxide using MoS₂ modified glassy carbon electrodes, *Mater. Lett.* 301 (2021) 130258, <https://doi.org/10.1016/j.matlet.2021.130258>.
- [41] I.I. Samoilenko, E.I. Vasil'eva, I.B. Pavlova, M.A. Tumanian, Mechanisms of the bactericidal action of hydrogen peroxide, *Zh. Mikrobiol. Epidemiol. Immunobiol.* 12 (1983) 30–33.
- [42] H. Jia, Y. Cai, J. Lin, H. Liang, J. Qi, J. Cao, W. Fei, Heterostructural graphene quantum dot/MnO₂ nanosheets toward high-potential window electrodes for high-performance supercapacitors, *Adv. Sci.* 5 (2018) 1700887, <https://doi.org/10.1002/adv.201700887>.
- [43] D.L. Angel, U. Fiedler, N. Eden, N. Kress, D. Adelung, B. Herut, Catalase activity in macro-and microorganisms as an indicator of biotic stress in coastal waters of the eastern Mediterranean Sea, *Helgol. Mar. Res.* 53 (1999) 209–218, <https://doi.org/10.1007/s101520050025>.
- [44] F.A.A. Alatrakchi, Rapid measurement of the waterborne pathogen *Pseudomonas aeruginosa* in different spiked water sources using electrochemical sensing: towards on-site applications, *Measurement* 195 (2022) 111124, <https://doi.org/10.1016/j.measurement.2022.111124>.
- [45] B. Serra, M.D. Morales, J. Zhang, A.J. Reviejo, E.H. Hall, J.M. Pingarron, In-a-day electrochemical detection of coliforms in drinking water using a tyrosinase composite biosensor, *Anal. Chem.* 77 (2005) 8115–8121, <https://doi.org/10.1021/ac051327r>.
- [46] K. Ishiki, D.Q. Nguyen, A. Morishita, H. Shiigi, T. Nagaoka, Electrochemical detection of viable bacterial cells using a tetrazolium salt, *Anal. Chem.* 90 (2018) 10903–10909, <https://doi.org/10.1021/acs.analchem.8b02404>.
- [47] D. Türkmen, T. Yilmaz, M. Bakhshpour, A. Denizli, An alternative approach for bacterial growth control: *pseudomonas* spp. imprinted polymer-based surface plasmon resonance sensor, *IEEE Sensor. J.* 22 (2021) 3001–3008, <https://doi.org/10.1109/JSEN.2021.3139509>.
- [48] J. Sun, A.R. Warden, J. Huang, W. Wang, X. Ding, Colorimetric and electrochemical detection of *Escherichia coli* and antibiotic resistance based on ap-Benzoquinone-Mediated bioassay, *Anal. Chem.* 91 (2019) 7524–7530, <https://doi.org/10.1021/acs.analchem.8b04997>.
- [49] R. Sivash Moakhar, T. Abdel Fatah, A. Sanati, M. Jalali, S.E. Flynn, S.S. Mahshid, S. Mahshid, A nanostructured gold/graphene microfluidic device for direct and plasmonic-assisted impedimetric detection of bacteria, *ACS Appl. Mater. Interfaces* 12 (2020) 23298–23310, <https://doi.org/10.1021/acsami.0c02654>.
- [50] K. Balaji Viswanath, N. Krithiga, A. Jayachitra, A.K. Sheik Mideen, A.J. Amali, V.S. Vasantha, Enzyme-free multiplex detection of *Pseudomonas aeruginosa* and *Aeromonas hydrophila* with ferrocene and thionine-labeled antibodies using ZIF-8/Au NPs as a platform, *ACS Omega* 3 (2018) 17010–17022, <https://doi.org/10.1021/acsomega.8b02183>.
- [51] Y.M. Kang, M.K. Kim, K.D. Zoh, Effect of nitrate, carbonate/bicarbonate, humic acid, and H₂O₂ on the kinetics and degradation mechanism of Bisphenol-A during UV photolysis, *Chemosphere* 204 (2018) 148–155, <https://doi.org/10.1016/j.chemosphere.2018.04.015>.
- [52] E. Abascal, L. Gómez-Coma, I. Ortiz, A. Ortiz, Global diagnosis of nitrate pollution in groundwater and review of removal technologies, *Sci. Total Environ.* 810 (2022) 152233, <https://doi.org/10.1016/j.scitotenv.2021.152233>.
- [53] B. Arumugam, V. Nagarajan, J. Annaraj, K. Balasubramanian, S. Palanisamy, S.K. Ramaraj, M. Chiesa, Synthesis of MnO₂ decorated mesoporous carbon nanocomposite for electrocatalytic detection of antifungal drug, *Microchem. J.* 182 (2022) 107891, <https://doi.org/10.1016/j.microc.2022.107891>.
- [54] L. Fiore, V. Mazaracchio, P. Galloni, F. Sabuzi, S. Pezzola, G. Matteucci, F. Arduini, A paper-based electrochemical sensor for H₂O₂ detection in aerosol phase: measure of H₂O₂ nebulized by a reconverted ultrasonic aroma diffuser as a case of study, *Microchem. J.* 166 (2021) 106249, <https://doi.org/10.1016/j.microc.2021.106249>.